JOURNAL OF Applied Polymer SCIENCE

Mechanically Adaptive Cellulose-Poly(acrylic acid) Polymeric Composites in Wet–Dry Cycles

Hongsheng Luo,[1] Jinlian Hu,[1] Yong Zhu,[1] Jian-Yong Wu,[2] Sheng Zhang,[3] Ying Fan,[3] Guangdou Ye[3]

[1]Institute of Textiles and Clothing, The Hong Kong Polytechnic University, Kowloon, Hong Kong, People's Republic of China

[2]Department of Applied Biology and Chemical Technology, The Hong Kong Polytechnic University, Kowloon, Hong Kong, People's Republic of China

[3]State Key Laboratory of Polymer Materials Engineering (Sichuan University), Polymer Institute of Sichuan University, Chengdu 610065, People's Republic of China

Correspondence to: J. Hu (E-mail: tchujl@inet.polyu.edu.hk)

ABSTRACT: Polymeric composites consisting of cellulose and poly(acrylic acid) (PAA) are prepared by coagulation/bulk polymerization method. Scanning electron microscopy and thermal gravimetric analysis are used to investigate the homogeneity and the heat-induced water loss of the composites, respectively. The water absorbed in the composites has strong hydrogen bonding with the polymer chains, as determined by differential scanning calorimetry. The mechanical and structural properties of the composites vary reversibly when the composites are applied into specifically explored wet–dry cycles, which are comprehensively measured by dynamic mechanic analysis, wide-angle X-ray diffraction, and Fourier transform infrared. It is unprecedented to explore the cellulose-PAA composites as a mechanical adaptive material. The cellulose and the PAA chemically react with each other. Most of the cellulose content remains in amorphous state. Thus, the water molecules can diffuse into the composites, leading to the wet–dry mechanical adaptability of the composites. © 2012 Wiley Periodicals, Inc. J. Appl. Polym. Sci. 000: 000–000, 2012

KEYWORDS: mechanically adaptive; cellulose; composites; wet–dry; hydrogen bonding

Received 7 May 2011; accepted 6 April 2012; published online
DOI: 10.1002/app.37851

INTRODUCTION

Cellulose, the most abundant natural polymer, has been attracting tremendous scientific and technological interests over the past several decades.[1] The cellulose features hydroxyl side groups and semirigid backbone in molecular structure. Strong hydrogen bonding among the hydroxyl groups lead to complex supramolecular structures, i.e., various polymorphous crystalline structures.[2,3] The crystalline structures endow the natural cellulose with unique properties, including extraordinary resistance to most organic solvents and poor elasticity in contrast to synthetic polymers.[4] Composites/blending methods have been widely used to explore cellulose-based polymeric materials with new properties which are originally absent for the natural cellulose.[5,6] Compared with physical blending of the cellulose with some paired polymers, chemical synthesis of semi-interpenetrating network (semi-IPN) provides ample possibilities to develop composites with dramatically improved mechanical properties and homogeneity.[7,8] It has shown that the cellulose plays the role of a matrix, and inside its physical network, a second network is formed in the semi-IPN structure. The composites commonly implement an optimum combination of functional properties of all IPN components: high mechanical strength and elasticity of the amorphous cellulose matrix. Various semi-IPN composites based on the cellulose have been reported, including cellulose-poly(2-hydroxyethylmethacrylate),[7] cellulose-poly(*N*, *N*-dimethylacrylamide),[8] and cellulose-poly(acrylamide-acrylic acid).[9] Recently, Yang et al. gave a review on the topic of the combination of polymeric hydrogels and porous membranes.[10] Structural and functional diversities were achieved by the use of a wide range of synthetic monomers and biopolymers. In addition, a new chelating IPN, achieved through blending of poly (acrylamide-*co*-acrylic acid) with newspaper pulp, was reported to have great performance for removal of copper metal ions.[11] However, there has been a very limited amount of literature on cellulose-based smart polymeric materials so far. In 2007, Aoki et al. reported a modified cellulose acetate (CA) with mercapto groups which exhibited shape memory behaviors due to the reversible crosslinking through adequate redox treatments.[12] A

novel mechanically adaptive polymeric nano-composite was developed by Capadona and coworkers who made good use of the hydrogen bonding among the cellulose nanowhiskers which reversibly stimulated by solvents.[13,14]

This article presents the first investigation on the cellulose-poly(acrylic acid) (PAA) semi-IPN composites as a smart material. Wet–dry mechanical adaptability was achieved for the composites. The cellulose and the PAA chemically reacted with each other. Most of the cellulose remained in amorphous state. Thus, water molecules were easy to diffuse into the composites, disrupting the hydrogen bonding previously existing among the polymer chains. The reversible stimulation of the hydrogen bonding by water led to the mechanical adaptability of the composites in the wet–dry cycles. Unlike other types of hydrogels, the explored cellulose-PAA composites maintained satisfactory modulus of around 1 MPa even in the wet state, which may attribute to the semirigid backbone of the cellulose constrained in the IPN structure. The combination of the modulus variation and the mechanical properties in both the wet and the dry states makes the cellulose-PAA be a candidate of the water-responsive shape memory composites.[15,16] The possible applications include biological or industrial components required to have the water-induced mechanical adaptability while maintaining certain mechanical strength. Furthermore, these findings may benefit for the development of smart materials based on natural polymers.

EXPERIMENTAL

Materials

The cellulose material employed was softwood sulfite dissolving pulp consisting of cellulose with a weight-average molecular weight of 9.82×10^5. *N, N*-dimethylacetamide (DMAc, anhydrous, 99.8%) obtained from Sigma-Aldrich chemical company (HongKong/PR China) as high-performance liquid chromatography (HPLC) grade, was dried over 4 Å molecular sieves, and was used without further purification. LiCl (Merck), obtained as p.a. grade, was dried under vacuum at 180°C for 1 day and stored in a glove box. Acrylic acid (AA; Aldrich Chemicals) was distilled under a vacuum before use. *N, N′*-Methylenebisacrylamide (MBA, Aldrich Chemicals, HongKong/PR China) was used as received. Ammonium persulfate ($(NH_4)_2S_2O_8$, Aldrich Chemicals) was recrystallized from water before use as the initiator of polymerization.

Preparation of Cellulose-PAA Composite Networks

Homogeneous solution with 2 wt % cellulose in DMAc/LiCl was obtained following the previous literature.[17,18] The regenerated cellulose films in pieces were prepared by casting 5 g of the cellulose solution on a clean glass plate and subsequently coagulating it with ethanol cautiously at each time. The obtained films were washed in distilled water for 24 h to remove the residual solvent and Li^+ ion, and then immersed into aqueous solution containing AA at 50 wt % and MBA at 0 wt %, 2 wt %, 5 wt %, and 15 wt %. To initiate the free-radical polymerization, $(NH_4)_2S_2O_8$ was used at a concentration of 0.5 wt %.[7,19] The films, allowed to swell for 10 min in the reaction solution to the degree of equilibrium swelling, were placed between two glass plates, pressed with clamps, and thermostated at 70°C. Free-radical polymerization started after an induction period of 10–15 min and was completed in 2 h. The obtained composite films were washed with distilled water for 8 h to remove low molecular weight impurities and dried to constant weight.

The composites are denominated by the letters "C" and "PA," which represent the cellulose and the PAA contents, respectively. The numbers followed "CPA" show the weight percentages of MBA in the composites. Pure regenerated cellulose film, named as "rC," is the control sample.

Characterizations

Scanning Electron Microscopy. A JEOL JSM-6490 scanning electronic microscopy (SEM) instrument was used to investigate the morphologies of the film samples. The cross-section of the samples broken in liquid nitrogen was coated with gold on JEOL JFC-1100E ion sputter coater in advance. The SEM micrographs were obtained by using 7 kV secondary electrons.

Thermal Gravimetric Analysis. Thermogravimetric analysis (TGA, Netzsch STA449C) with Argon as the purge gas for the swollen samples were carried out in the range of room temperature and 200°C at the rate of 10 °C min^{-1}. The samples were immersed into distilled water for 1 h and then were compressed gently between two tissues to remove the excess water prior to the TGA tests.

Differential Scanning Calorimetry. The freezing point depression and the melting point elevation of the bound water in the composites were investigated by differential scanning calorimetry (DSC, Perkin-Elmer Diamond) with nitrogen as purge gas in a program including cooling (Perkin-Elmer, Intra-cooler II) and subsequent heating. Indium and zinc standards were used for calibration. The temperature program was set to cool from room temperature to −70°C at −10 °C min^{-1} and subsequent heating from −70°C to room temperature at 10 °C min^{-1}.

Dynamic Mechanic Analysis. Dynamic mechanical analysis (DMA) was performed by using a Perkin–Elmer instrument at frequency of 2 Hz. All samples, in the size of 15 mm × 10 mm × 0.8 mm (length × width × height), were immersed into water to swell prior to the tests. In the DMA tests, the samples experienced two successive states of "wet" and "partially dry" by immersion into water for around 20 min or heating from room temperature to 90°C within around 20 min. Each sample was heated and immersed three times in the cycles. The reversible modulus changes of the samples versus time were recorded.

Fourier Transform Infrared and X-Ray Diffraction. Fourier transform infrared (FTIR) spectra and Wide-angle X-ray scattering diffraction (WXRD) of the samples in both wet and dry states were obtained by using a Perkin–Elmer System 2000 FT-IR spectrophotometer and Rigaku RINT 2200V. For WXRD, the diffracted intensity of Cu KR radiation (wavelength of 0.1542 nm, under a condition of 40 kV and 30 mA) was measured in a 2θ range between 5° and 40°.

RESULTS AND DISCUSSION

Preparation and Morphology of the Composites

The molecular structures of cellulose, AA, and MBA are shown in Figure 1. The optical image of the wet regenerated cellulose film from coagulation is shown in Figure 2(a). The rC film was optically clear and gel-like in appearance, indicating that most

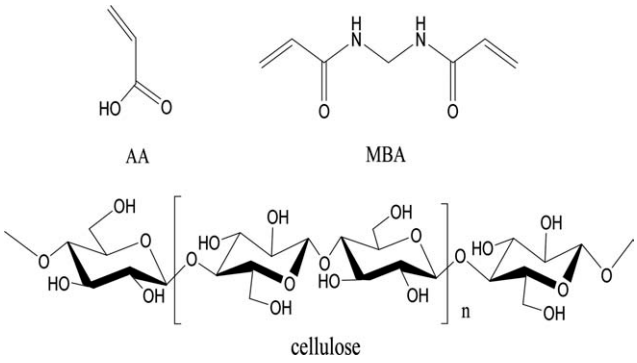

Figure 1. Molecular structures of AA, MBA, and cellulose.

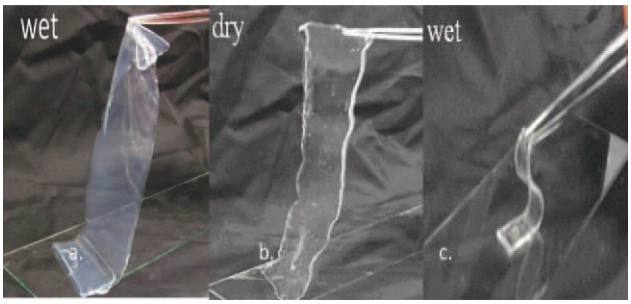

Figure 2. Optical images of regenerated cellulose (a) and cellulose-PAA composites in the dry (b) and the wet (c) states. [Color figure can be viewed in the online issue, which is available at wileyonlinelibrary.com.]

cellulose was in amorphous state. The loose and amorphous structure allowed the monomers to diffuse into the matrix of the film easily when the rC films were immersed into the reaction solution containing AA and MBA. $(NH_4)_2S_2O_8$ was used to initialize the polymerization of the monomers absorbed in the gel, generating cellulose semi-IPN. Figure 2(b) shows the optical image of the cellulose-PAA composite in the dry state. The composite film kept transparency like rC. The dry composite films were rather rigid, suggesting that they had remarkably high modulus. The composite films decreased the modulus, became elastic and stretchable when they were immersed into water for several minutes. A small piece of the cellulose-PAA composite was cut and swollen in water. The optical image of the stretched piece is shown in Figure 2(c).

Figure 3 shows the SEM images of the surface (a) and the bulk (b) morphology of sample CPA5. The morphologies for other composite specimens were similar as that of CPA5. Neither phase separation nor obvious aggregates in microscale could be observed for CPA5. The coagulation/polymerization method allowed better homogeneity to achieve for the resultant composites compared to those from physical blending. Previous research on cellulose-poly(acryloyl morpholine) composites, performed by Miyashita et al., even shown that this type of IPN-like composites were substantially homogeneous on a scale of a few nanometers.[19] In contrast to the physical blends of cellulose with polyamide 66[20] or poly(vinyl pyrrolidone)[21] where aggregates or crystalline in the size of about 1 μm could be found, the IPN-like cellulose composites could dramatically improve their mechanical properties due to their homogeneity.

Thermogravimetic Analysis

Figure 4 shows the plots of the residual weights of the composites against temperature. Each wet-state sample lost its primary water content with the increase of the temperature in the range of 50–100°C. The residual weights approached to constant as the temperature increased above 100°C. The percentages of the residual weights against the initial weights of the wet-state composites were found to depend on the compositions, being at most 56% for CPA15 and at least 18% for rC. The chemical crosslinker MBA may enhance the crosslinking density of the semi-IPN structure in the composites, leading to less free volume for the water molecules to be absorbed by the composites. Furthermore, increase of the temperature from room temperature to around 90°C within 20 min enabled the swollen samples to lose more than 70 percentage of the water content. Thus, a heating program with the same temperature range and heating rate as that in the TGA tests was applied for the wet and the partially dry states transition of the composites in the subsequent wet–dry cyclic measurements.

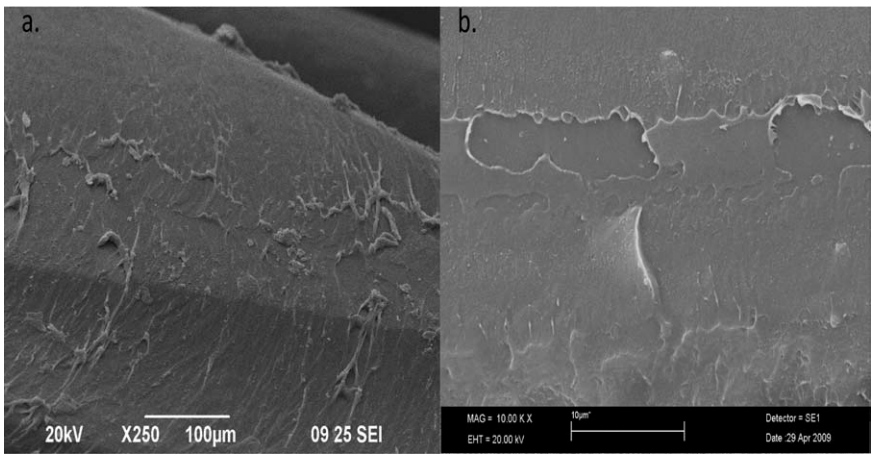

Figure 3. SEM images of the surface (a) and the bulk (b) morphology of CPA5.

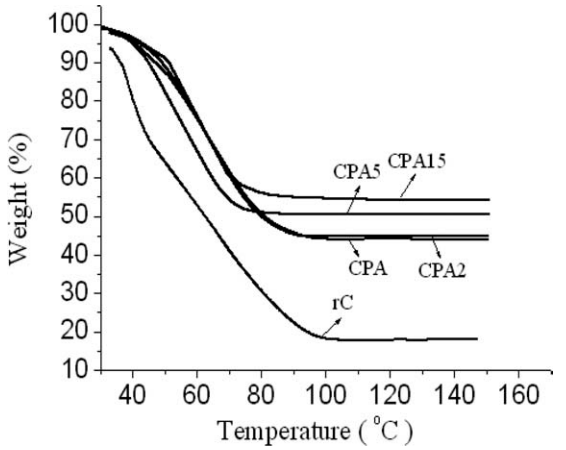

Figure 4. Plots of residual weight of the composites against temperature.

DSC Measurements

The thermograms of the swollen composites in temperature scan were investigated by subambient DSC. Sharp peaks located in the range −14.69°C to −21.14°C were observed (shown in Figure 5) in the cooling process from the room temperature to −70°C at the rate of −5 °C min^{-1}. The peaks could be assigned as the exothermic freezing of the absorbed water in the samples. The location of the peaks was the lowest −21.14°C for CPA15 whereas the highest −14.69°C for rC. Additionally, the melting points of absorbed water were elevated, as determined in the heating program from −70°C to the room temperature at the rate of 5°C min^{-1} (shown in Figure 6). The melting points shifted upwards with the increase of the MBA contents in the composites, being −0.11°C for rC, 1.90°C for CPA, 2.62°C for CPA2, 3.40°C for CPA5, and 5.41°C for CPA15. The similar phenomenon of the freezing points depression was reported for many other polymer–water systems including selected starch- and cellulose-based polymeric hydrogels[22] and cellulose-poly (vinyl alcohol) blends.[23] The water molecules absorbed in the composites could be divided into two parts, namely the free water and the bound water. The variation in both the freezing and the melting points may attribute to strong hydrogen bonding between the bound water and the polymer matrix. Furthermore, the effect of the hydrogen bonding on the thermal transitions of the absorbed water was found to be amplified for the composites with higher MBA content. The crosslinking of the composites may increase with the increase of the MBA content. As a result, the percentage of the bound water against the overall absorbed water in the composites increased correspondingly, leading to the amplified deviation in the thermal transition temperatures.

Reversible Modulus Variation of the Composites in the Wet–Dry Cycles

Luo et al. specifically explored a thermal-aqueous programming to stimulate triple-shape effect of a novel cellulose-based polymeric nano-composite.[24] Similarly, a wet–dry cycle was applied to the cellulose-PAA composites which showed reversible variation in the storage modulus. Figure 7 shows the plots of the modulus of the composites against time in the cycles. The wet-state samples showed relatively lower modulus, which kept at constant with small fluctuation in the initial stage of the tests. Subsequently, the samples gradually increased their modulus during the process of water evaporation induced by heating. Each sample approached to maximum modulus when the temperature was up to 90°C. According to the TGA curves, the composites were estimated to lose more than 70 percentage of the water content upon exposure of the aforementioned thermal treatment. This state was "partially dry-state." The modulus of samples encountered pronounced decrease as the partially dry-state samples were immersed into water for several minutes (wet-state). The states transition along with modulus variation was repeatedly conducted for three times. Dashed lines in the Figure 7 were used to separate the heating and the immersion process. The neat sample rC was found to have the wet-state modulus of around 1.1 MPa and the dry-state modulus of around 1.6 MPa. All the cellulose-PAA composites had higher modulus even in the wet-state compared to rC, indicative of the mechanical improvement due to the semi-IPN structure. Additionally, the modulus of composites both in wet and dry states increased with the increase of the MBA content. The composites had much more wet–dry modulus contrast compared to the neat sample rC. For instance, the modulus contrast was 9.3 for

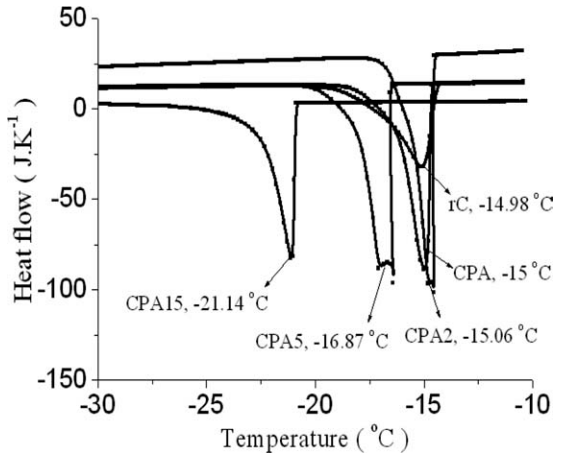

Figure 5. Thermogram of composites against temperature in the cooling process.

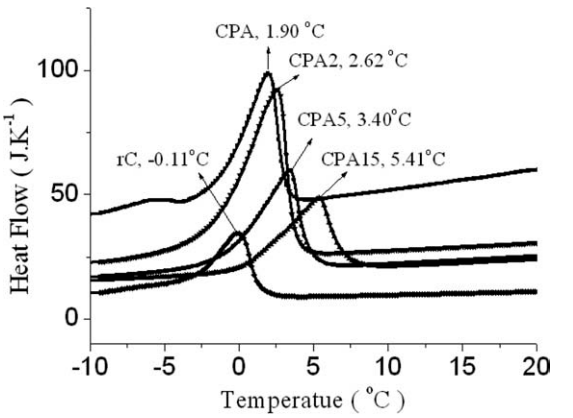

Figure 6. Thermogram of composites against temperature in the heating process.

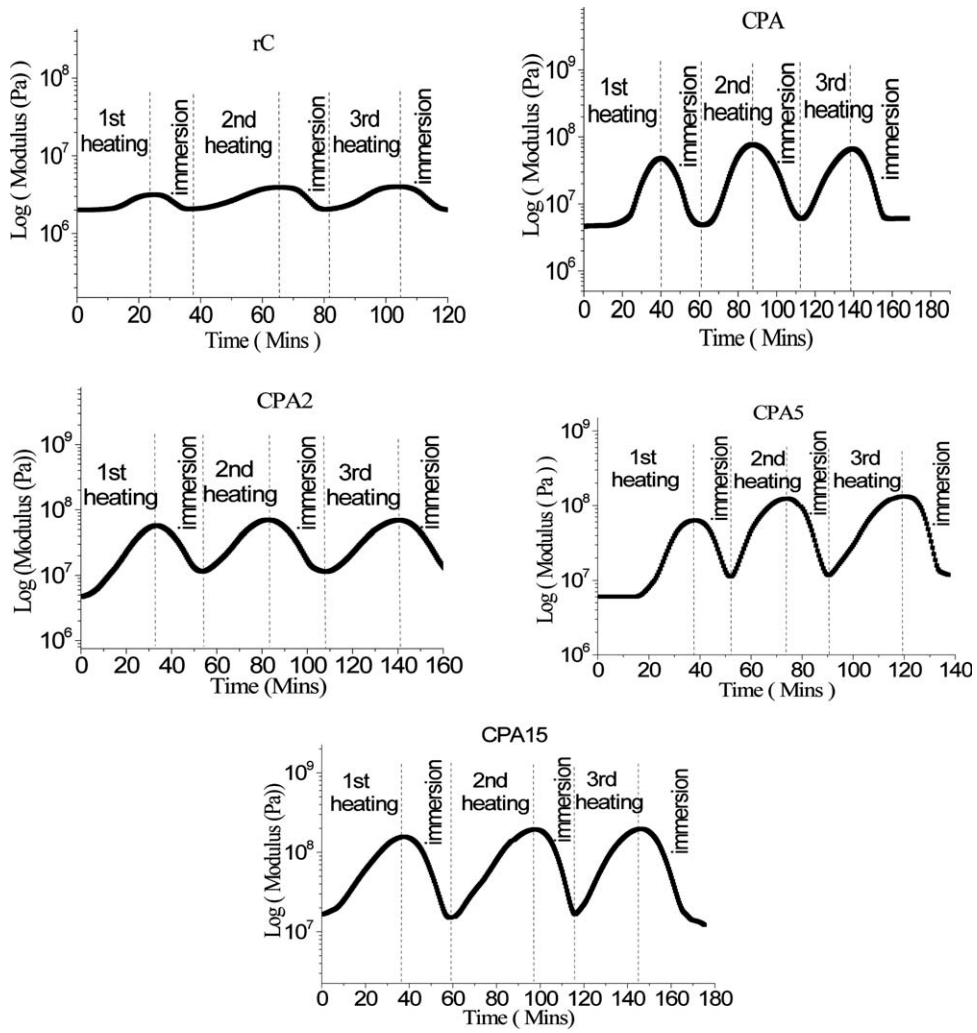

Figure 7. Plots of storage modulus of the composites against time in the wet–dry cycles.

CPA having the wet-state modulus of 1.4 MPa and the dry-state modulus of 13 MPa and increased to 9.6 for CPA15 possessing the wet-state modulus of 11 MPa and the dry-state modulus of 105 MPa. It has been known that water affected the structure and the relaxation behavior of the cellulose quite seriously.[25,26] Particularly, the modulus of the cellulose remarkably decreased due to the plasticization effect of the absorbed water.[27,28] In this study, the absorbed water may play not only a role as a plasticizer, but also hydrogen bonding competitive reagent. The swollen composites, compared with the partially dry-state composites, had relatively lower modulus because the latter contained much more hydrogen bonding among the polymers.

Reversible Structural Variation of the Composites in the Wet–Dry Cycles

The WXRD profiles of the raw material cellulose pulp and the neat sample rC in both the wet and the dry states are shown in Figure 8. The cellulose pulp had much higher intensity than that of the rC. Two broad diffraction peaks with the centre location at 27.8° and 8.17° were observed. However, there were no obvious peaks in diffraction profiles of the rC, except for a broad peak centrally located at around 18.44° as the rC was in the dry state. Combined with the previous X-ray diffraction investigation on the cellulose,[29,30] it could be concluded that the microstructure of the cellulose varied depending on the

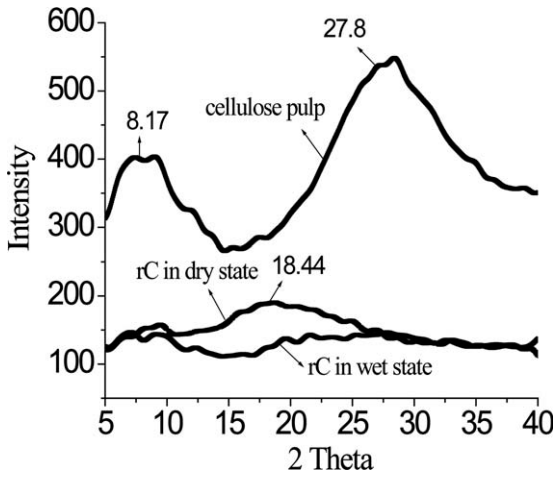

Figure 8. WXRD profiles of cellulose pulp and rC in the wet and the dry states.

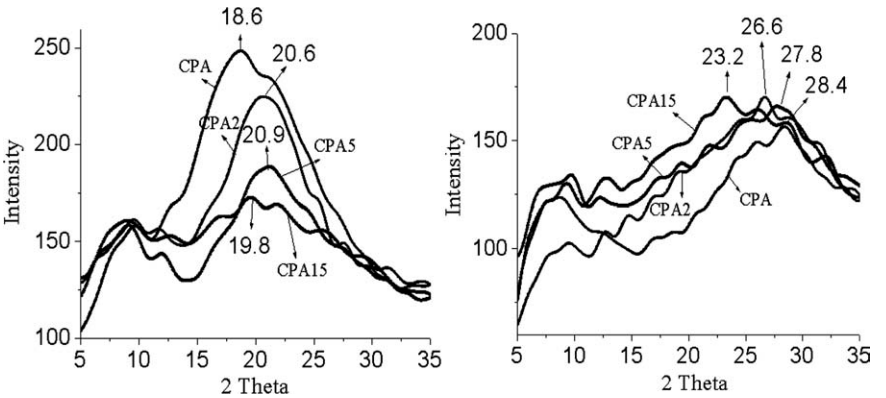

Figure 9. WXRD profiles of cellulose-PAA composites in the wet (left) and the dry (right) states.

resources, dissolution–regeneration treatment, and humidity conditions. It was reported that the crystalline scatter of 22.5° for cellulose crystalline I or of 19.8° for crystalline II.[31,32] Thus, the diffraction peak in the profile of the dry-state rC suggested that the dry-state rC had a complex condense structure being similar to crystalline II. Figure 9 shows the WXRD profiles of the cellulose-PAA composites. The wet-state composites had broad diffraction peaks in the range 23.2–28.4° which shifted to the range 18.6–20.9° when the composites were transferred into the dry state. The different profiles of the composites in the wet and the dry states provided clear evidence that the microstructure of the composites varied during the state transition. Furthermore, most of the cellulose may remain in the amorphous state because sharp crystalline diffraction peaks were absent in the profiles of the composites. Figures 10 and 11 show the FTIR spectra of the cellulose-PAA composites. A broad peak with the central location at 3353.9 cm^{-1} appeared for each wet-state composite, associating with the hydroxyl groups bound with water.[33,34] The peaks shifted to 2941.2 cm^{-1} and became much sharper when the specimens were subjected to thermal treatment. In the region of 2000–650 cm^{-1}, the band locating at 1714 cm^{-1} could be designated as the —C=O group of the PAA content in the composites. Additionally, the band located at 1172 cm^{-1} was assigned as ester group —C(=O)—O, proving that the PAA not only physically blended, but also chemically reacted with the cellulose by the ester formation reaction between the carboxyl groups and the hydroxyl groups. The chemical reaction between the two polymers may increase the crosslinking density of the composites. The proposed semi-IPN structure of the cellulose-PAA composites is schematically illustrated in Scheme 1. The cellulose and the PAA formed a microscale homogenous network chemically crosslinked by the ester bonds. Most of the cellulose was in the amorphous state. The water was easy to diffuse in the amorphous structure of the composites, disrupting the hydrogen bonding previously existing among the polymers. The microstructure of the composites reversibly varied during the wet and the dry states transition, leading to mechanical adaptability in the wet–dry cycles.

CONCLUSIONS

Cellulose-PAA composites in semi-IPN structure were microscale homogeneous. The composites exhibited mechanical adaptability when applied into specifically explored wet–dry cycles. The cellulose and the PAA contents chemically reacted with each other. Most of the cellulose was in amorphous state. Water was able to diffuse into the composites, disrupting the

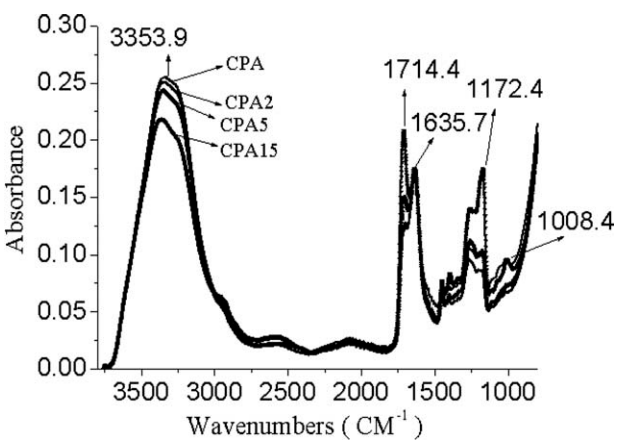

Figure 10. FTIR spectrum of the composites in the wet states.

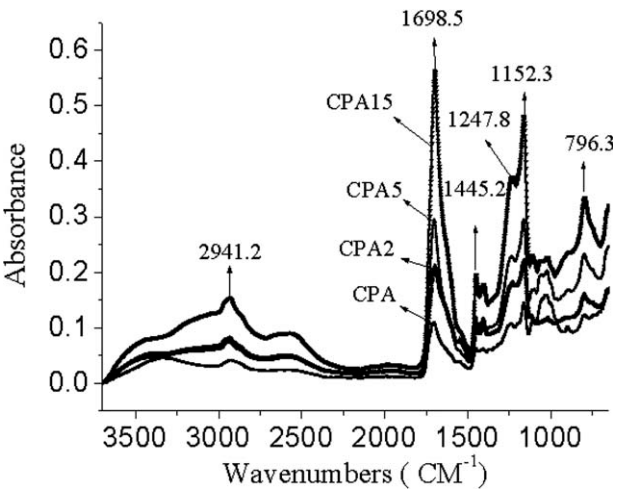

Figure 11. FTIR spectrum of the composites in the dry states.

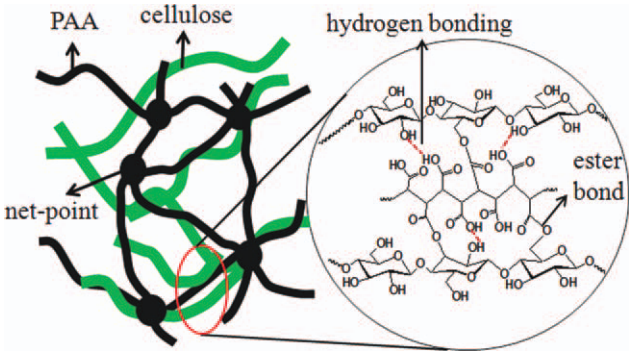

Scheme 1. Proposed semi-IPN structure of the cellulose-PAA composites. [Color figure can be viewed in the online issue, which is available at wileyonlinelibrary.com.]

hydrogen bonding of the polymer chains. Correspondingly, the microstructure of the composites reversibly varied during the wet and the dry states transition, leading to the mechanical adaptability in the wet–dry cycles.

ACKNOWLEDGMENTS

This project was supported by Hong Kong Research Grants Council project (RGC-GRF/518209), Hong Kong ITF research project GHS/088/04, GHP/045/07TP, the Niche Area Fund of Hong Kong Polytechnic University (J-BB6M), and the Opening Project of Polymer Materials Engineering State Key Laboratory (Sichuan University) (200803).

REFERENCES

1. Klemm, D.; Heublein, B.; Fink, H. P.; Bohn, A. *Angew. Chem. Int. Ed.* **2005,** *44*, 3358.
2. Kadla, J. F.; Gilbert, R. D. *Cell Chem. Technol.* **2000,** *34*, 197.
3. Kim, N. H.; Imai, T.; Wada, M.; Sugiyama, J. *Biomacromolecules* **2006,** *7*, 274.
4. Ramos, L. A.; Assaf, J. M.; El Seoud, O. A.; Frollini, E. *Biomacromolecules* **2005,** *6*, 2638.
5. Marsano, E.; Corsini, P.; Canetti, M.; Freddi, G. *Int. J. Biol. Macromol.* **2008,** *43*, 106.
6. Nishio, Y.; Manley, R. *Macromolecules* **1988,** *21*, 1270.
7. Nishio, Y.; Hirose, N. *Polymer* **1992,** *33*, 1519.
8. Williamson, S.; Armentrout, R.; Porter, R.; McCormick, C. *Macromolecules* **1998,** *31*, 8134.
9. Buyanov, A.; Revel'skaya, L.; Kuznetzov, Y.; Shestakova, A. J. *Appl. Polym. Sci.* **1998,** *69*, 761.
10. Yang, Q.; Adrus, N.; Tomicki, F.; Ulbricht, M. J. *Mater. Chem.* **2011,** *21*, 2783.
11. Haroun, A. A.; El-Halawany, N. R. *Polym. Plast. Technol.* **2011,** *50*, 232.
12. Aoki, D.; Teramoto, Y.; Nishio, Y. *Biomacromolecules* **2007,** *8*, 3749.
13. Shanmuganathan, K.; Capadona, J. R.; Rowan, S. J.; Weder, C. J. *Mater. Chem.* **2010,** *20*, 180.
14. Capadona, J. R.; Shanmuganathan, K.; Tyler, D. J.; Rowan, S. J.; Weder, C. *Science* **2008,** *319*, 1370.
15. Chen, S. J.; Hu, J. L.; Chen, S. G.; Zhang, C. L. *Smart Mater. Struct.* **2011,** *20*, 065003.
16. Chen, S. J.; Hu, J. L.; Zhuo, H. T. *J. Mater. Sci.* **2011,** *46*, 6581.
17. McCormick, C. L.; Callais, P. A.; Hutchinson, B. H. *Macromolecules* **1985,** *18*, 2394.
18. Chrapava, S.; Touraud, D.; Rosenau, T.; Potthast, A.; Kunz, W. *Phys. Chem. Chem. Phys.* **2003,** *5*, 1842.
19. Miyashata, Y.; Kimura, N.; Suzuki, H.; Nishio, Y. *Cellulose* **1998,** *5*, 123.
20. Garciaramirez, M.; Cavaille, J. Y.; Dupeyre, D.; Peguy, A. J. *Polym. Sci. Part B Polym. Phys.* **1994,** *32*, 1437.
21. Paillet, M.; Cavaille, J. Y.; Desbrieres, J.; Dupeyre, D.; Peguy, A. *Colloid Polym. Sci.* **1993,** *271*, 311.
22. Faroongsarng, D.; Sukonrat, P. *Int. J. Pharm.* **2008,** *352*, 152.
23. Radloff, D.; Boeffel, C.; Spiess, H. W. *Macromolecules* **1996,** *29*, 1528.
24. Luo, H. S.; Hu, J. L.; Zhu, Y. *Macromol. Chem. Phys.* **2011,** *212*, 1981.
25. Schartel, B.; Wendling, J.; Wendorff, J. *Macromolecules* **1996,** *29*, 1521.
26. Yano, S.; Hatakeyama, H. *Polymer* **1988,** *29*, 566.
27. Myllytie, P.; Salmen, L.; Haimi, E.; Laine, J. *Cellulose* **2010,** *17*, 375.
28. Zhou, S.; Tashiro, K.; Hongo, T.; Shirataki, H.; Yamane, C.; Ii, T. *Macromolecules* **2001,** *34*, 1274.
29. Moharram, M. A.; Mahmoud, O. M. *J. Appl. Polym. Sci.* **2007,** *105*, 2978.
30. Oh, S.; Yoo, D.; Shin, Y.; Kim, H.; Kim, H.; Chung, Y.; Park, W.; Youk, J. *Carbohydr. Res.* **2005,** *340*, 2376.
31. Mansikkamaki, P.; Lahtinen, M.; Rissanen, K. *Cellulose* **2005,** *12*, 233.
32. Yokochi, H. C. A. A. *J. Appl. Polym. Sci.* **2000,** *76*, 1466.
33. Kondo, T. *Cellulose* **1997,** *4*, 281.
34. Kondo, T.; Sawatari, C. Polymer (London) **1996,** *37*, 393.